Water Supply

IWA PUBLISHING

Water Supply Vol 22 No 4, 4262 doi: 10.2166/ws.2022.048

Establishing a statistical relation between meteorological and hydrological drought indices

M. A. Jincy Rose and N. R. Chithra

Department of Civil Engineering, National Institute of Technology, Calicut, India
*Corresponding author. E-mail: jincy.rose.ma@gmail.com

MAJ, 0000-0001-9104-8090

ABSTRACT

Investigation of the hydrological drought behaviour of the Bharathapuzha river basin of Kerala, India, on account of the meteorological drought condition of the watershed was carried out in this study with the aid of four popular drought indices. Statistical relations were established between the indices using polynomial regression models to help in predictions. A study on the decadal spatial variation of hydrological drought behaviour over the basin was also conducted. The cross-correlation study was also performed to understand the propagation of hydrological drought in the event of meteorological drought. The results reveal a slight decrease in the spatial extent of hydrological drought over time. The correlation between meteorological and hydrological drought indices was found to be more assertive at grid locations G1 and G4. According to the findings, the strongest correlation of 0.8 in the propagation of meteorological to hydrological drought was observed at a lag of 3 months over a 12 -month timescale. Run theory reveals that the river basin is subjected to hydrological drought over 54–65% of the months in the historic period. Regression analysis suggests that the cubic model outperforms the other models.

Key words: cross-correlation, hydrological drought, meteorological drought, polynomial regression, run theory, spatial variation

HIGHLIGHTS

- Four distinct drought indices were used to identify drought characteristics.
- Spatiotemporal drought patterns were analysed in a tropical river basin in Kerala, India.
- The propagation of meteorological to hydrological drought was obtained through a cross-correlation study.
- Establishes a statistical relation between meteorological and hydrological drought indices.

GRAPHICAL ABSTRACT

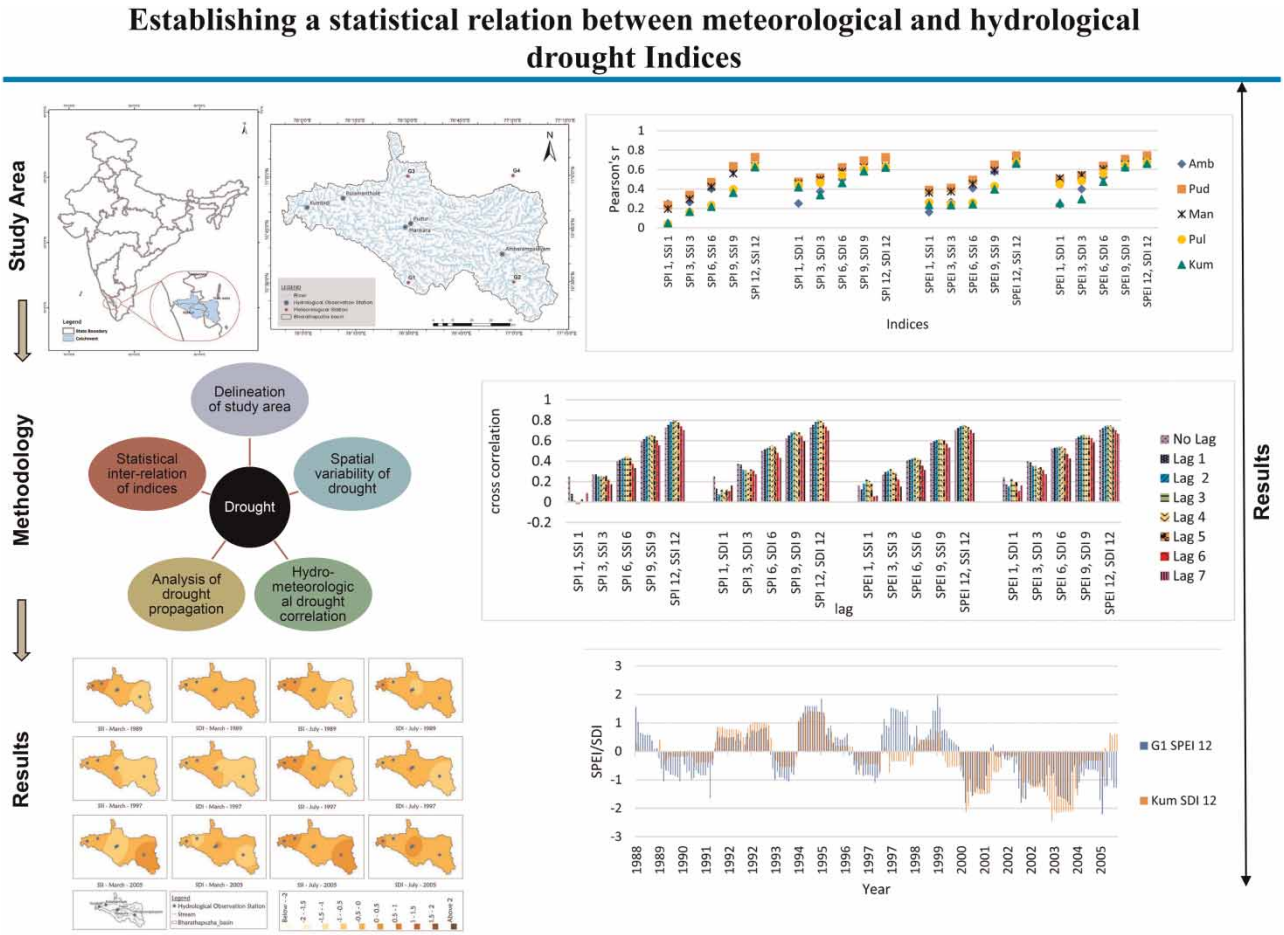

INTRODUCTION

Drought and water crisis are two of the most pressing, costlier, and damaging issues humanity has faced in recent years (Lindsay *et al.* 2017). Droughts are classified according to the cause of their occurrence, with meteorological, hydrological, agricultural, and socioeconomic droughts being the most common (Mishra & Singh 2010). The primary reason for the repeating extreme event of drought is reduced precipitation over a long period, ranging from several months to a year (Dai 2011), leading to deficiencies in surface and subsurface water, and affecting agricultural productivity and socio-economic stability. There are several definitions for each of the drought classifications, but there is a lack of unanimity on the definition of drought itself due to its varied nature (Van Loon 2015).

Hydrological droughts are significant among these categories due to the reliance of many anthropogenic activities on surface water resources (Vasiliades *et al.* 2011). They are also more noticeable than other types of droughts. According to Mishra *et al.* (2019), hydrological droughts are significant because they directly impact the water supply system, resulting in less agricultural productivity and may lead to famine in the worst-case scenario. As a result, it is critical to investigate the elements that influence the occurrence of hydrological droughts to appropriately handle drought-related calamities (Vidal *et al.* 2010).

Droughts are monitored using a variety of indicators to alleviate them (Eslamian *et al.* 2017). The popular meteorological and hydrological indices widely used in India include the Standardised Precipitation Index (SPI), Standardised Evapotranspiration Index (SPEI), Standardised Streamflow Index (SSI), and Streamflow Drought Index (SDI) (Wable *et al.* 2019). River flows, rainfalls, reservoir levels, soil moisture, groundwater levels, rate of evapotranspiration, and other parameters subsumed in these indices may be used to assess the severity of a drought (McCleskey *et al.* 2010). Compared to other meteorological indices, probability distribution functions are involved in the computation of SPI and SPEI, which are capable

of displaying meteorological drought characteristics and are hence referred to as standard indices for analysing meteorological drought in various parts of the world (Lotfirad *et al.* 2022). Meteorological droughts occur in India frequently due to climate change (Mishra *et al.* 2020), and hydrological events are followed by meteorological drought episodes (Wilhite 2000). Drought propagation studies, which provide the time it takes for a meteorological to hydrological drought translation, are therefore critical for water planners (Apurv *et al.* 2017). Previous research in the subject area has shown an upward trend in temperature and a downward trend in precipitation over time (Rose & Chithra 2020). This complicates analysing hydrological droughts with streamflow as a function of precipitation, evaporation, and temperature (Mazrooei *et al.* 2015).

Past studies have explored different aspects of drought propagation and forecasting techniques using Cross wavelet analysis (Li *et al.* 2020a, 2020b), hydrological modeling (Ahmadalipour *et al.* 2017), and correlation among the drought characteristics between SPI value time series at various time intervals (Edossa *et al.* 2010). There are studies on building relationships among the various drought indices with a focus on drought characteristics. For instance, Salimi *et al.* (2021) established a relation between the duration and severity of drought indices using non-linear models.

Bharathapuzha is the largest river basin in Kerala, a once perennial and lifeline river which has experienced drought and water scarcity in recent decades. No other study in this regard on the tropical river basin is available. Also, this is a data-sparse location with considerable damming (11 dams) in a short 209 km river, and building hydrological models is time-consuming and likely to be erroneous. As a result, statistical research is the best alternative. The study was carried out assuming that the current river flow conditions and reservoir operation policies will continue in the future. In light of the preceding literature, the purpose of this research was (1) to understand the hydrological drought condition of the basin, (2) to investigate the drought propagation pattern of the river basin, and (3) to develop a statistical relationship between meteorological and hydrological drought indices. This research will help in the timely management of surface water, groundwater, agriculture, and livelihood. This study contributes to comprehensive drought studies, which help establish a statistical relation between meteorological and hydrological droughts.

MATERIALS AND METHODS

Study area and data

This study is conducted in the Bharathapuzha river basin, which runs along India's Kerala-Tamil Nadu border. The river takes its origin at an altitude of 2,250 m above mean sea level in the Anamalai Hills in the state of Tamil Nadu and flows into the Arabian Sea in Ponanni in Kerala. Gayathripuzha, Chitturpuzha, Kalpathipuzha, and Thuthapuzha are the primary tributaries of the Bharathapuzha river. The Bharathapuzha river gets its name from the confluence of the Kalpathipuzha and the Chitturpuzha near Parali. The geographical coordinates of the river basin stretch between latitude 10°26′ to 11°13′ N and longitude 75°53′ to 77°13′ E. The overall length of the river from its source to its mouth is roughly 209 km, and it drains a total area of 6,186 km^2, with 71% of it falling within Kerala and the rest in Tamil Nadu. The Bharathapuzha basin, located in the rain shed zone of the Western Ghats, receives a generous amount of rain during the southwest monsoon. The river basin receives an annual average rainfall of 1,132 mm each year. The basin's average annual streamflow is 45.87 cumecs (45.87 m^3/s), while the minimum and maximum temperatures are 12.8 and 36 °C respectively. The temperature in the basin varies according to the season as it is located in a tropical region. Various literature describes that the watershed suffers a water-stressed condition (Drissia 2019). This information alludes to the need to investigate the basin's hydrological drought issues.

This study makes use of rainfall, temperature, and streamflow data for a historic period (1988–2005). The meteorological indices SPI and SPEI are calculated from gridded precipitation (0.5°×0.5°) and gridded temperature (1°×1°) data from the Indian Meteorological Department (IMD). The grids are denoted as G1, G2, G3, and G4. The streamflow data provided by the Central Water Commission (CWC) of India is freely available (https://indiawris.gov.in/wris/#/RiverMonitoring) and is used to generate the hydrological indices, SSI and SDI. Ambarampalayam (Amb), Pudur (Pud), Mankara (Man), Pulamanthole (Pul), and Kumbidi (Kum) are the hydrological stations. As the percentage of missing data in the time series is less than 3, a simple linear interpolation approach was used to fill in the gaps. The location of the study area along with the hydrological and meteorological locations in the study area is given in Figure 1. Information on hydrological and meteorological stations is presented in Tables 1 and 2.

Estimation of drought indices

McKee *et al.* (1993) and Vicente-Serrano *et al.* (2010) established SPI and SPEI, which are two frequently used multi-scalar drought indices. These indexes are primarily used to detect meteorological drought in a given area. Other factors, such as soil

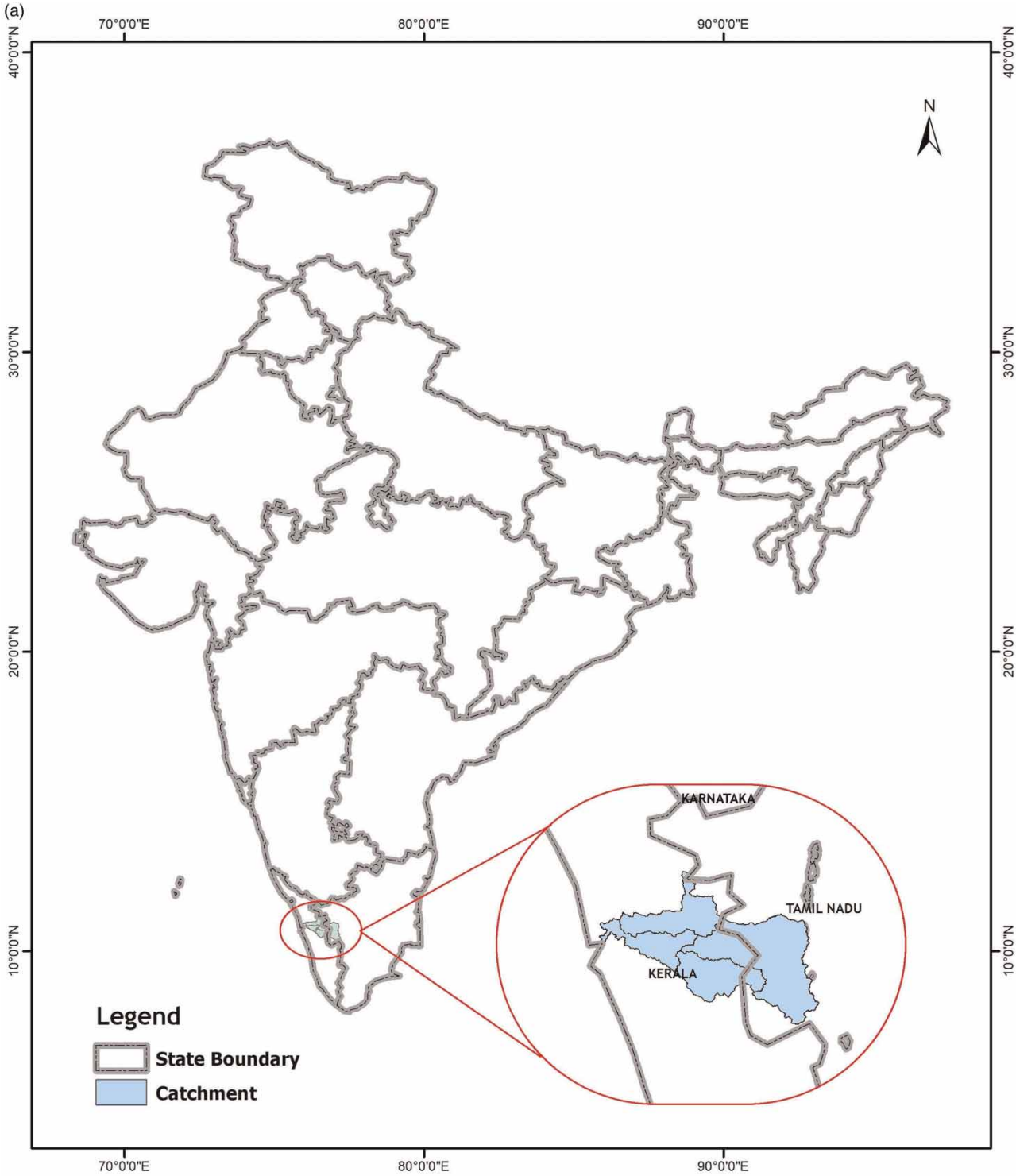

Figure 1 | (a) Location map of the study area (b) Meteorological and hydrological locations in the study area. (*Continued*).

moisture at shorter durations (3 months) and hydrological conditions at longer timescales (12 months), can also be captured from these indices. In SPI computation, the probability of observed precipitation is turned into a simple index with precipitation as the single input parameter. The long-term precipitation time series is fitted mostly to a gamma distribution or Pearson type III distribution. It is then transformed to a normal distribution with mean zero and standard deviation of

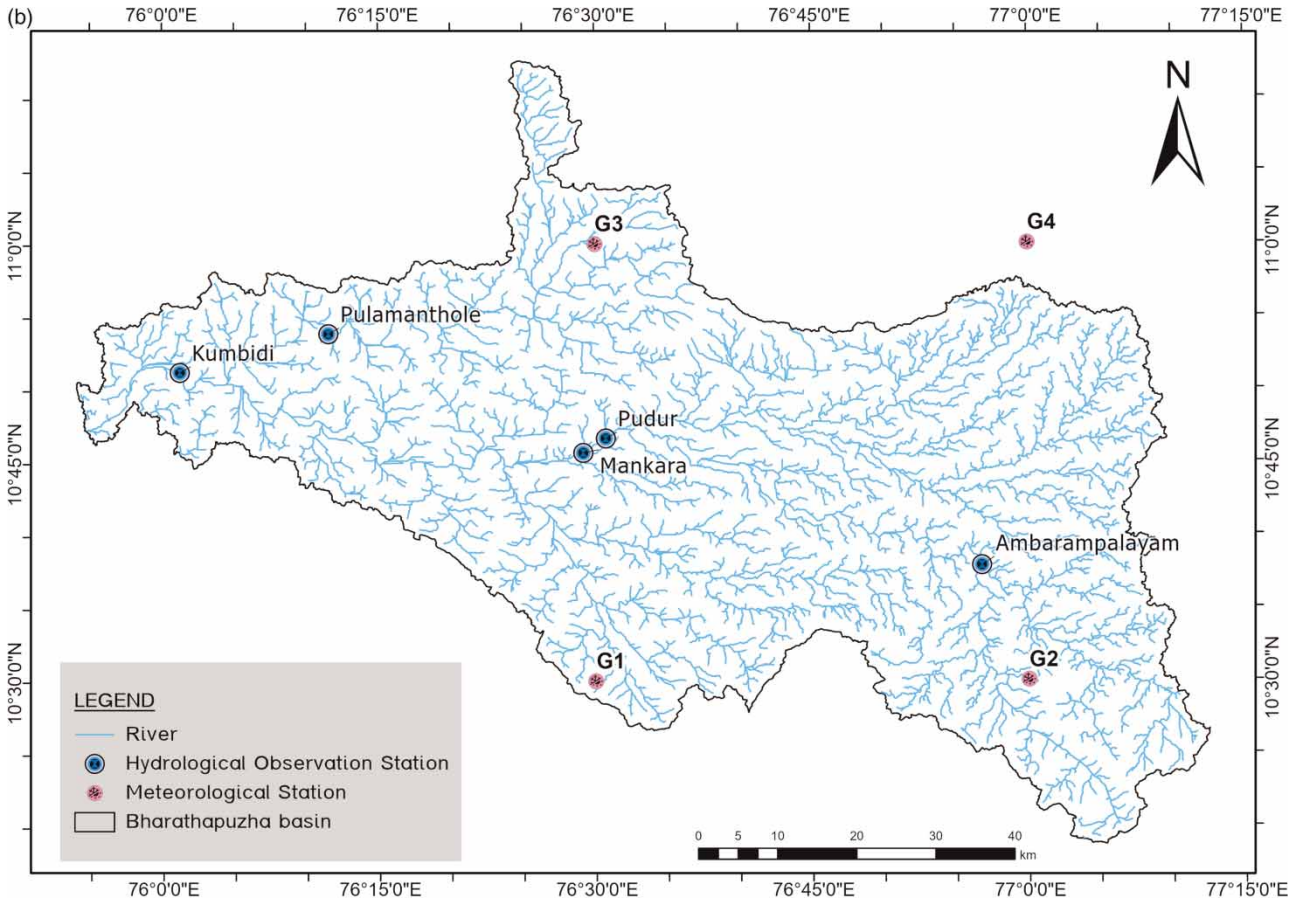

Figure 1 | Continued.

Table 1 | Information on the hydrological stations

Site name	Catchment area (sq.km)	Latitude (N)	Longitude (E)	Elevation
Ambarampalayam	950	10°37′49″	76°56′46″	218 m
Pudur	1,313	10°46′48″	76°34′30″	62 m
Mankara	2,775	10°45′40″	76°29′10″	40 m
Pulamanthole	940	10°53′57″	76°11′50″	8 m
Kumbidi	5,755	10°51′00″	76°01′12″	2 m

Table 2 | Information on the Meteorological stations

Grid	Latitude (N)	Longitude (E)	Elevation
G1	10°30′0″	76°30′0″	292 m
G2	10°30′0″	77°0′0′	418 m
G3	11°30′0″	76°30′0″	101 m
G4	11°30′0″	77°0′0’	397 m

one. The normalised SPI values are seen as standard deviations from the median. Thus, wet and dry periods can be represented in the same way. The standard deviations higher than or less than the median precipitation explain the wet or dry condition respectively. SPEI is computed based on temperature and precipitation data, which assesses the effect of temperature variability in drought. SPEI is calculated using a climatic water balance equation, which takes into account the difference between precipitation and potential evapotranspiration (PET). The Thornthwaite equation is used to calculate PET in this investigation. Rose & Chithra (2020) explains a comparative examination of the meteorological indices for the study area and describes the comprehensive approach adopted.

The computation of both SDI developed by Nalbantis & Tsakiris (2009) and SSI introduced by Modarres (2007) requires only the streamflow values. Furthermore, the approach used by these indices is statistically similar to that used by SPI. SDI computes the cumulative flow rate of a river $Q_{i,j} = \sum_{j=1}^{3k} q_{i,j}$ where, $q_{i,\,j}$ refers to the total streamflow volumes for the i^{th} hydrological year and the k^{th} timeframe; 'j' attributes the months, with values ranging from 1 for September to 12 for August. There are four timeframes: October–December, October–March, October–June, and October–September, with the numbers 1, 2, 3, and 4 respectively. Using the cumulative streamflow volume for each time frame of k in the i^{th} hydrological year, SDI is calculated as follows:

$$SDI_{i,k} = \frac{Q_{i,k} - \overline{Q_k}}{S_k} \tag{1}$$

where $\overline{Q_k}$ and S_k are the mean and standard deviation, respectively, of the cumulative volume of the streamflow during the time frame of k and over a long period. Although SDI is similar to river standardised streamflow volume, this analysis uses mean river flow rate data. SSI has a similar theoretical background as that of SPI. The only difference is that instead of precipitation data, streamflow data are used. The monthly flow value aggregate is used to calculate SSI, whereas SDI is computed for each reference period as mentioned above. Following the actual definitions, SPEI uses a log-Logistic distribution by default, and SPI, SSI, and SDI use a Gamma distribution. However, a detailed analysis of the parameter distributions of the indices can also be investigated, as in the study of Malik *et al.* (2021). The drought indices used in this study share a common drought classification, as given in Table 3.

Inverse distance weighting (IDW) interpolation

The rationale behind IDW interpolation is that points near together are more comparable than those farther away. It uses the known values surrounding the prediction point to compute the value of any point that is not quantified. The data points closest to the prediction point have a stronger influence than those further away. As a result, it is assumed that each data point exhibits a localised effect that increases in close proximity. The IDW approach gets its name because it gives more weight to locations closer to the forecast (Katipoğlu *et al.* 2021).

The equation is as follows:

$$W_i = \frac{\frac{1}{d_i^p(x_i)}}{\sum_{i=1}^{n} \frac{1}{d_i^p(x_i)}} \tag{2}$$

Table 3 | Drought Classification (McKee *et al.* 1993)

Index Value	Category
2.00 or greater	Extremely wet
1.50 to 2.00	Severely wet
1.00 to 1.50	Moderately wet
0 to 1.00	Near normal (mildly wet)
0 to − 1.00	Near normal (mild drought)
−1.00 to −1.50	Moderate drought
−1.50 to −2.00	Severe drought
−2.00 or lower	Extreme drought

$$\hat{Z}(x_0) = \sum W_i Z(x_i) \tag{3}$$

$$\sum_{i=1}^{n} W_i = 1 \tag{4}$$

where, x_0 is the prediction point, $\hat{Z}(x_0)$ is the prediction value at x_0, $Z(x_i)$ is the value of the sample point at x_i, W_i is the IDW of the sample at x_i comparison to x_0, d is the proximity between the sample point and the prediction point, p is the power parameter, and n is the number of data points to be considered in the computation around the prediction point.

Statistical analysis

The study performs a Pearson correlation analysis and cross-correlation function over the indices and the efficiency of the mathematical relationship between the indices is established by the coefficient of determination (R^2).

Cross-correlation function

The cross-correlation function determines how similar a time-series data is to lagged forms of another time-series data as a function of lag. Assume that the time series y_{1a} and y_{2a} have lags l, where $l = 0, 1, 2, \ldots$. Cross-correlation may be calculated for data pairs (y_{11}, y_{21}), (y_{12}, y_{22}), (y_{1N}, y_{2N}) using sample standard deviations and the lag l cross-covariance as follows:

$$S_{y1} = \sqrt{C_{y1y2}(0)};\ C_{y1y2}(0) = Var(y_1) \tag{5}$$

$$S_{y2} = \sqrt{C_{y2y2}(0)};\ C_{y2y2}(0) = Var(y_2) \tag{6}$$

$$r_{y1y2}(l) = \frac{C_{y1y2}(l)}{S_{y1}S_{y2}};\ l = 0, \pm 1, \pm 2, \ldots \tag{7}$$

The lag l cross-covariance, sample standard deviations, and cross-correlation are represented by C_{ymyn}, S_{ym}, and r_{ymyn}, respectively.

Regression equations

Polynomial regression is a regression algorithm that models the relationship between the regressor x and the regressand y as an nth degree polynomial in x. Linear, quadratic and cubic regressions are commonly used polynomial regressions. Linear regression is a linear model that assumes a linear relationship between the input variable (x) and the output variable (y). It is of the form, $y = a + bx + e$, where a and b are regression coefficients and e is the error variable, an unobserved random variable that is assumed to be independently and identically distributed with zero mean and constant variance. Quadratic regression and cubic regression are of the form, $y = a + bx + cx^2 + e$, and $y = a + bx + cx^2 + dx^3 + e$, respectively, where a, b, c, and d are regression coefficients and e is the error variable.

RESULTS AND DISCUSSION

Spatial variability of hydrological drought in the study area

As seen in Figure 2, the lighter shade denotes an extreme drought situation. Over the years, a slight decrease in the severity of hydrological drought is found both during the summer and monsoon months of the year. The dry eastern part of the basin gets wetter over the period. Compared to the monsoon months of the years, the summer period experiences a slightly higher drought severity, which explains the seasonal drought behavior of the river basin. Comparing the summer and monsoon months, it is evident that the downstream shows a wetter state during the monsoon, whereas it is relatively dry during the summer months. This demonstrates the impact of human interference, particularly the influence of a dam on the flow pattern. The overall root mean squared error (RMSE) statistic obtained from the cross-validation procedure is 0.61 for SDI and 0.39 for SSI.

Meteorological and hydrological drought correlation

Figure 3 depicts the Pearson correlation (r) between SPI-SSI, SPI-SDI, SPEI-SSI, and SPEI-SDI throughout time steps of 1–12 months. A measure of strength and direction of association between continuous variables is obtained here. The value of r ranges from −1 to 1. A value of 1 indicates a perfect positive correlation stating that a hydrological drought will occur

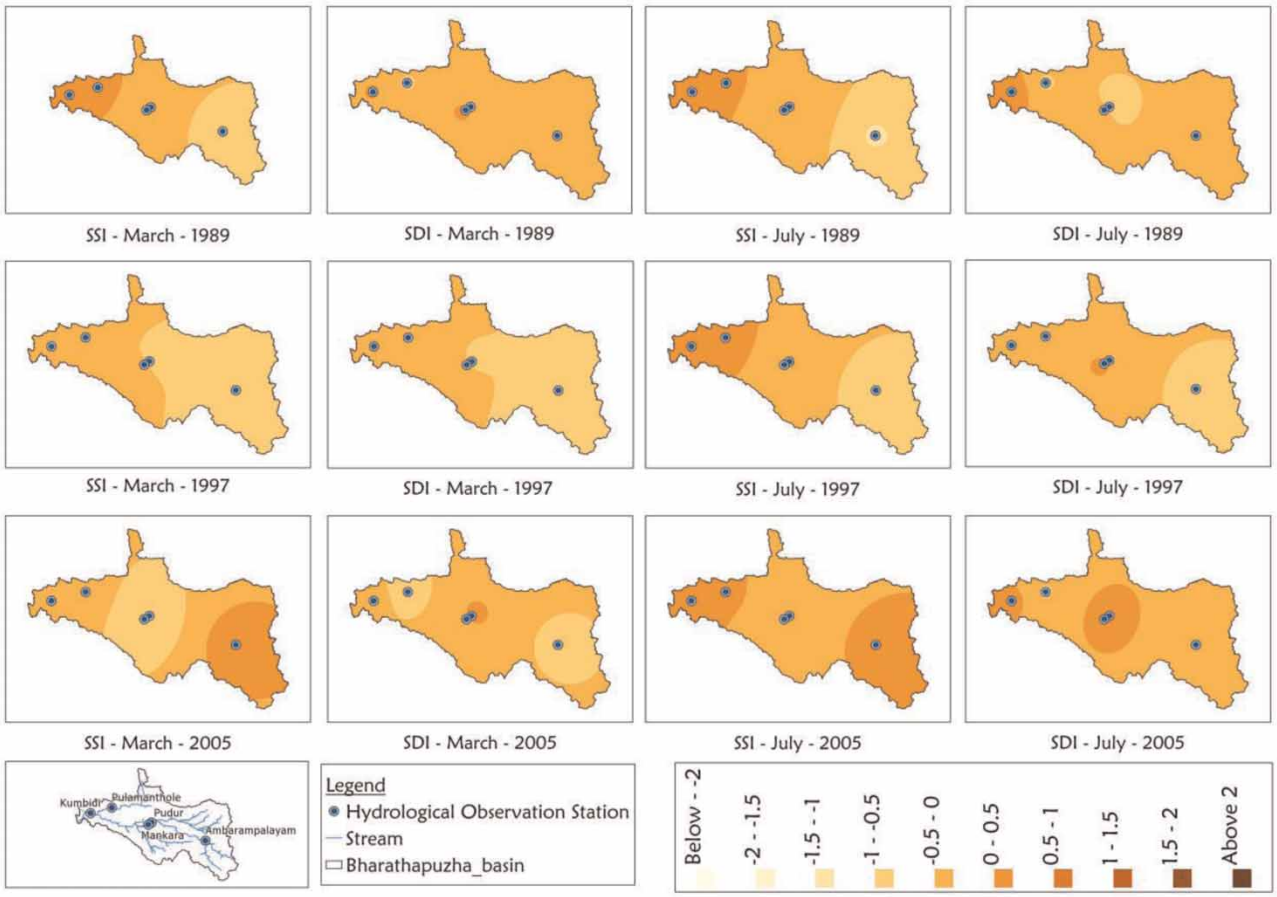

Figure 2 | Spatial plot of SSI and SDI with the decadal variation of indices in summer (March) and Monsoon (July) during 1988–2005.

on the occurrence of a meteorological drought event, whereas a value of −1 indicates a perfect negative correlation among the indices. Positive and negative signs imply the direction of relation: positive values denote that both variables move in the same direction. Negative values explain that they move in the opposite direction (when one increases, the other decreases or vice versa). At G1, the correlation between all the meteorological and hydrological indices increases with the timescale, where the highest correlation is observed at the 12-month timescale. It is found that all the stations other than Ambarampalayam show an association of around 0.7 at G1. In G2, the association of SPI and SPEI with SDI decreases with timescale whereas a slight increase with SSI is observed. However, a correlation of below 0.6 with all the hydrological indices is observed. At G3, the correlation between meteorological and hydrological indices is low (r-value below 0.5) at all the hydrological stations and decreases with timescale. All the hydrological stations show a better correlation with G4, ranging from 0.61 to 0.73 at a 12-month timescale. Overall, G1 and G4 are highly associated with the hydrological stations.

Analysis of drought propagation

The highest cross-correlation observed among the meteorological and hydrological drought indices in the river basin is depicted in Figure 4 with a lag of up to 7 months, which is summarised in Table 4. Based on the results, the highest correlation obtained at Ambarampalayam is at a 3-month lag with a value of 0.8 at a 12-month timescale between the SPI and SSI indices. This explains that a hydrological drought will occur at Ambarampalayam with a 3-month lag period after the occurrence of a meteorological event at G4. Pudur shows the highest association of 0.74 with G4 with a zero-lag period at a 12-month timescale. Mankara, Pulamanthole, and Kumbidi are highly associated with G1 with values of 0.73, 0.8, and 0.71 respectively at a zero-lag period in a 12-month timescale. A zero-lag period explains that the hydrological drought is reflected immediately after the occurrence of a meteorological event. The temporal variations of high cross-over correlated meteorological and hydrological indices can be seen in Figure 5.

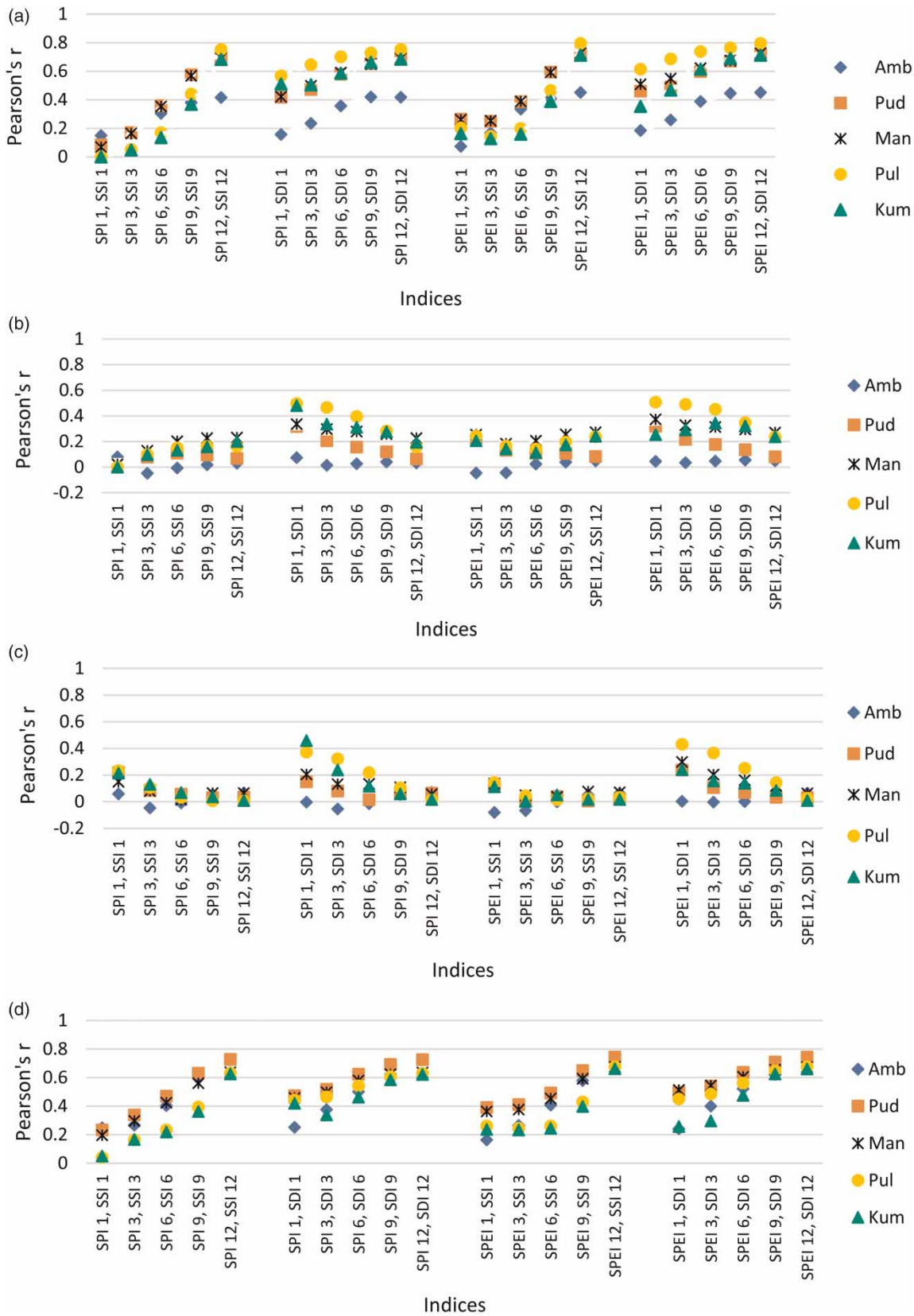

Figure 3 | 1–12-month Pearson correlation coefficients between indices at (a) G1 (b) G2 (c) G3 (d) G4.

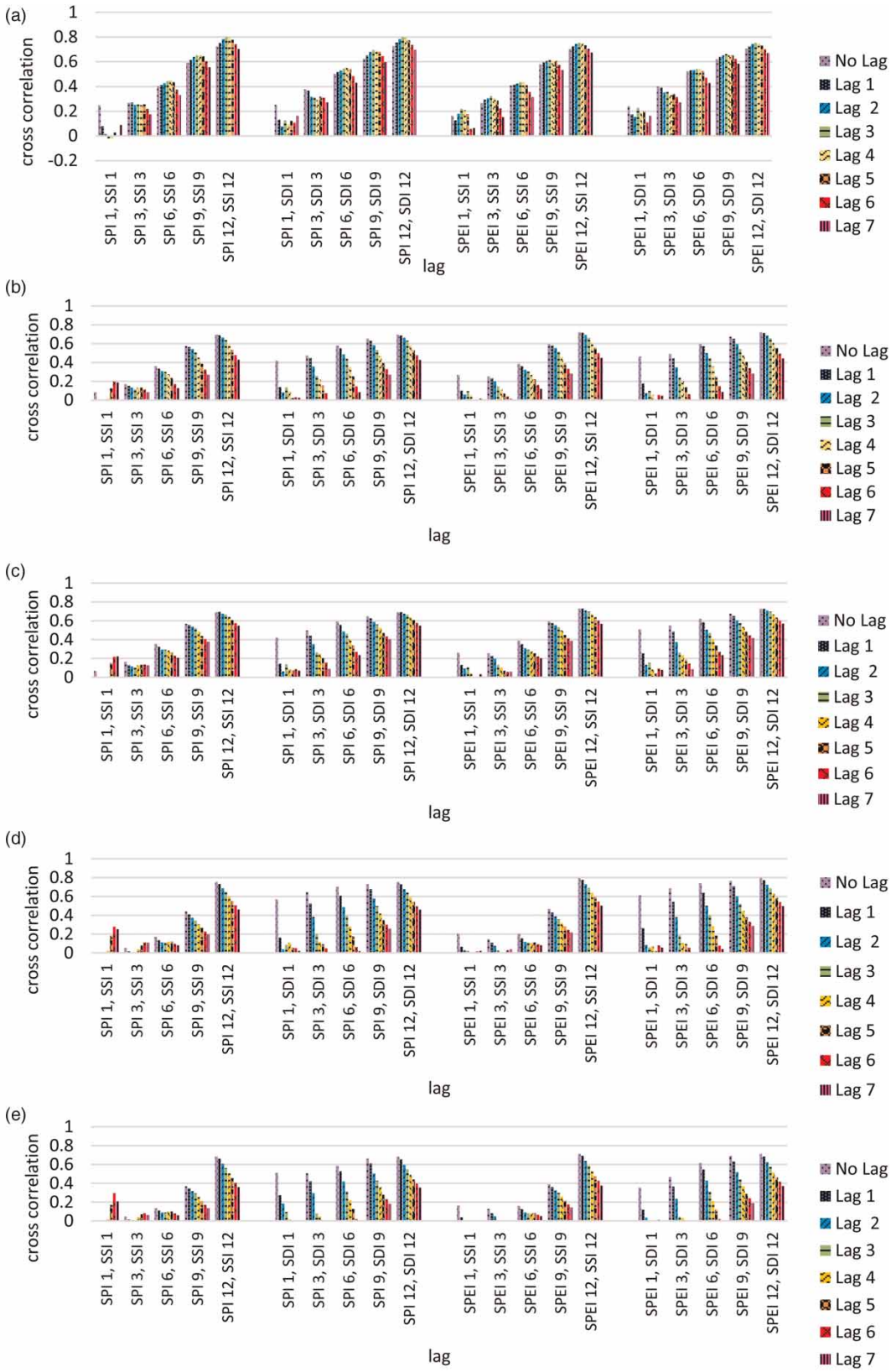

Figure 4 | Crossover correlation among the highly correlated combinations (a) G4 vs Ambarampalayam (b) G1 vs Pudur (c) G1 vs Mankara (d) G1 vs Pulamanthole (e) G1 vs Kumbidi.

Table 4 | Cross-correlation among the indices (ccf = cross-correlation function)

Meteorological stations		Hydrological Stations				
		Amb	Pud	Man	Pul	Kum
G1	Highest ccf	0.51	0.72	0.73	0.80	0.71
	Associated indices	SPEI, SDI	SPEI, SDI	SPEI, SDI	SPEI, SDI	SPEI, SDI
	Lag (months)	3	0	0	0	0
	Timescale (month)	12	12	12	12	12
G2	Highest ccf	0.17	0.32	0.37	0.51	0.48
	Associated indices	SPEI, SDI	SPEI, SDI	SPEI, SDI	SPEI, SDI	SPI, SDI
	Lag (months)	3	0	0	0	0
	Timescale (month)	1	1	1	1	1
G3	Highest ccf	0.2	0.3	0.3	0.4	0.5
	Associated indices	SPEI, SDI	SPEI, SDI	SPEI, SDI	SPEI, SDI	SPEI, SDI
	Lag (months)	5	7	0	0	0
	Timescale (month)	12	1	1	1	1
G4	Highest ccf	0.80	0.74	0.68	0.68	0.66
	Associated indices	SPI, SSI	SPEI, SSI	SPEI, SSI	SPEI, SSI	SPEI, SSI
	Lag (months)	3	0	0	0	0
	Timescale (month)	12	12	12	12	12

Drought characteristics using run theory

Based on run theory, Table 5 explains the highest drought severity and corresponding duration (months) experienced in each meteorological and hydrological location. It is found that the meteorological drought at G1 and G4 with the highest severity was observed between 2000 and 2004, whereas those at G2 and G3 occurred between 1988 and 1992. The severity of these events in the basin ranges from 40.17 to 67.43 with a duration spanning between 37 and 68 months. It is also noted that the river basin experienced an overall meteorological drought event between 54 and 65% of the months during the historical period 1988–2005. The most severe hydrological droughts occurred between the years 1988–1992 and 1999–2005, with magnitudes ranging from 40.5 to 85.53 and lasting 50 to 70 months. In the basin, an overall hydrological drought month accounted for 53% to 65% of the time.

Statistical interrelation of indices

In this study, linear, quadratic, and cubic polynomial regression models were fitted to pairs of indices (SPI-SSI, SPI-SDI, SPEI-SSI, SPEI-SDI) to establish statistical relations where the dependent variables - being the hydrological indices (y) - and the meteorological variables - being the independent variable (x) - were modeled as an nth degree polynomial in x. Better R^2 values were obtained for the cubic model, followed by quadratic and linear models. The cubic and quadratic models performed significantly better compared to the linear model. R^2 is calculated and tabulated in Table 6. All the R^2 values greater than 0.5 are given in the table. It is found that the highest R^2 value is obtained at Pulamanthole station against the G1 location between 12-month SPEI-SSI and SPEI-SDI and with a value of 0.65. Kumbidi, Pulamanthole, Mankara, and Pudur show an R^2 value ranging between 0.52 and 0.65 with the G1 location, and a value ranging between 0.52 and 0.55 is obtained for G4 location with Ambarampalayam, Pudur, and Pulamanthole stations.

On determining the meteorological drought in the study area, the statistical relationship established among the hydrometeorological indices helps anticipate a hydrological drought ahead of its occurrence. The insights found in this study could be an essential step in addressing drought susceptibility and help drought management measures for mitigation. Identifying regional vulnerabilities allows water planners and managers to formulate suitable mitigation strategies such as meticulous planning of water resources, changes in water-dependent industries, revamping of irrigation systems, and assisting decision-makers in considering drought from a hazard viewpoint and incorporating the notion of drought vulnerability into natural resource planning.

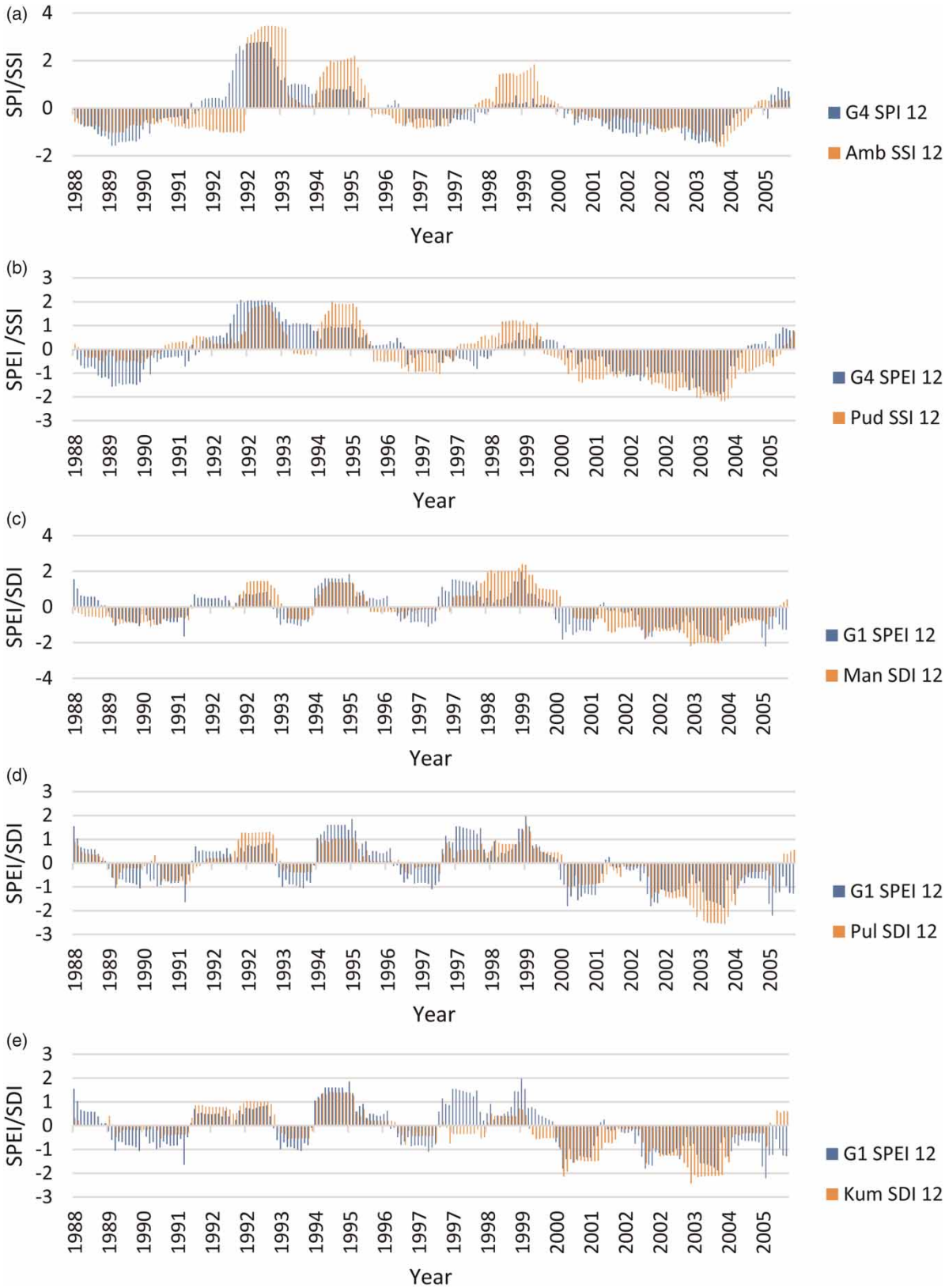

Figure 5 | Temporal variation of indices with the highest cross-correlation (a) Ambarampalayam (b) Pudur (c) Mankara (d) Pulamanthole (e) Kumbidi.

Table 5 | Highest drought severity and corresponding duration (months) experienced in each meteorological and hydrological location based on run theory

Location	Severity > 30	period	Corresponding Duration (months)	Total Drought duration (months)	Drought months (%)
Amb SDI 12	41.48	Sep 1988–Oct 1992	50	135	64.90
Amb SDI 12	40.50	Jul 2000–Jan 2005	55	135	64.90
Pud SDI 12	85.53	Dec 1999–Aug 2005	69	124	59.62
Man SDI 12	72.15	Oct 2000–Aug 2005	62	135	64.90
Pul SDI 12	65.42	Jun 2000–Aug 2005	63	110	52.88
Kum SDI 12	73.72	Sep 1999–Jun 2005	70	126	60.58
G1 SPEI 12	67.43	May 2000–Dec 2005	68	116	55.77
G2 SPEI 12	40.17	Sep 1988–Sep 1991	37	116	55.77
G3 SPEI 12	63.60	Sep 1988–Jul 1992	47	135	64.90
G4 SPEI 12	49.69	May 2000–Oct 2004	54	113	54.33

Table 6 | Statistical relations between the indices

Meteorological station	Hydrological station	Indexes	Relations	R^2
G1	Pud	SPEI-12, SSI-12	$SSI = -0.07 + 0.76\ SPEI$	0.521
			$SSI = -0.12 + 0.77\ SPEI + 0.05\ SPEI^2$	0.523
			$SSI = -0.12 + 0.79\ SPEI + 0.05\ SPEI^2 - 0.01\ SPEI^3$	0.523
		SPEI-12, SDI-12	$SDI = -0.11 + 0.77\ SPEI$	0.519
			$SDI = -0.15 + 0.77\ SPI + 0.05\ SPEI^2$	0.521
			$SDI = -0.15 + 0.80\ SPEI + 0.04\ SPEI^2 - 0.02\ SPEI^3$	0.521
	Man	SPI-12, SSI-12	$SSI = -0.06 + 0.99\ SPI + 0.07\ SPI^2 - 0.11\ SPI^3$	0.508
		SPEI-12, SSI-12	$SSI = 0.02 + 0.8\ SPEI$	0.53
			$SSI = -0.04 + 0.80\ SPEI + 0.07\ SPEI^2$	0.534
			$SSI = -0.03 + 0.92\ SPEI + 0.06\ SPEI^2 - 0.06\ SPEI^3$	0.538
		SPI-12, SDI-12	$SDI = -0.1 + 0.99\ SPI + 0.07\ SPI^2 - 0.11\ SPI^3$	0.505
		SPEI-12, SDI-9	$SDI = 0.8\ SPEI$	0.523
			$SDI = -0.08 + 0.8\ SPEI + 0.09\ SPEI^2$	0.528
			$SDI = -0.08 + 0.86\ SPEI + 0.08\ SPEI^2 - 0.03\ SPEI^3$	0.529
		SPEI-12, SDI-12	$SDI = -0.02 + 0.8\ SPEI$	0.529
			$SDI = -0.09 + 0.81\ SPEI + 0.07\ SPEI^2$	0.533
			$SDI = -0.08 + 0.93\ SPEI + 0.06\ SPEI^2 - 0.06\ SPEI^3$	0.537
	Pul	SPI-12, SSI-12	$SSI = 0.04 + 0.66\ SPI$	0.568
			$SSI = 0.08 + 0.65\ SPI - 0.04\ SPI^2$	0.57
			$SSI = 0.1 + 0.8\ SPI - 0.06\ SPI^2 - 0.07\ SPI^3$	0.58
		SPEI-12, SSI-12	$SSI = 0.06 + 0.71\ SPEI$	0.631
			$SSI = 0.15 + 0.70\ SPEI - 0.11\ SPEI^2$	0.644
			$SSI = 0.61 + 0.72\ SPEI - 0.11\ SPEI^2 - 0.01\ SPEI^3$	0.645
		SPI-6, SDI-6	$SDI = 0.08 + 0.67\ SPI - 0.11\ SPI^2$	0.507
			$SDI = 0.08 + 0.68\ SPI - 0.11\ SPI^2 - 0.01\ SPI^3$	0.508
		SPI-9, SDI-9	$SDI = -0.01 + 0.68\ SPI$	0.533
			$SDI = 0.10 + 0.68\ SPI - 0.12\ SPI^2$	0.553
			$SDI = 0.11 + 0.61\ SPI - 0.14\ SPI^2 + 0.03\ SPI^3$	0.555
		SPI-12, SDI-12	$SDI = -0.01 + 0.68\ SPI$	0.569
			$SDI = 0.03 + 0.68\ SPI - 0.04\ SPI^2$	0.572
			$SDI = 0.05 + 0.81\ SPI - 0.06\ SPI^2 - 0.06\ SPI^3$	0.579
		SPEI-6, SDI-6	$SDI = 0.7\ SPEI$	0.547
			$SDI = 0.14 + 0.7\ SPEI - 0.16\ SPEI^2$	0.572
			$SDI = 0.13 + 0.59\ SPEI - 0.15\ SPEI^2 - 0.06\ SPEI^3$	0.576
		SPEI-9, SDI-9	$SDI = 0.72\ SPEI$	0.585
			$SDI = 0.15 + 0.71\ SPEI - 0.16\ SPEI^2$	0.611

(*Continued*)

Table 6 | Continued

Meteorological station	Hydrological station	Indexes	Relations	R^2
			$SDI = 0.16 + 0.48\ SPEI - 0.18\ SPEI^2 + 0.13\ SPEI^3$	0.631
		SPEI-12, SDI-12	$SDI = 0.74\ SPEI$	0.634
			$SDI = 0.1 + 0.73\ SPEI - 0.11\ SPEI^2$	0.645
			$SDI = 0.1 + 0.74\ SPEI - 0.11\ SPEI^2 - 0.01\ SPEI^3$	0.645
	Kum	SPEI-12, SSI-12	$SSI = -0.06 + 0.61\ SPEI$	0.507
			$SSI = 0.04 + 0.6\ SPEI - 0.11\ SPEI^2$	0.522
			$SSI = 0.04 + 0.61\ SPEI - 0.11\ SPEI^2 + 0.004\ SPEI^3$	0.522
		SPEI-9, SDI-9	$SDI = 0.03 + 0.44\ SPEI - 0.16\ SPEI^2 + 0.1\ SPEI^3$	0.512
		SPEI-12, SDI-12	$SDI = -0.12 + 0.64\ SPEI$	0.508
			$SDI = 0.62 - 0.12\ SPEI + 0.62\ SPEI^2$	0.523
			$SDI = -0.02 + 0.62\ SPEI - 0.12\ SPEI^2 + 0\ SPEI^3$	0.523
G4	Amb	SPI-12, SSI-12	$SSI = 0.08 + 0.89\ SPI$	0.524
			$SSI = 0.07 + 0.88\ SPI + 0.01\ SPI^2$	0.524
			$SSI = 0.05 + 0.96\ SPI + 0.07\ SPI^2 - 0.03\ SPI^3$	0.526
		SPEI-12, SSI-12	$SSI = -0.07 + 0.87\ SPEI + 0.17\ SPEI^2$	0.519
			$SSI = -0.08 + 0.92\ SPEI + 0.18\ SPEI^2 - 0.02\ SPEI^3$	0.519
		SPI-12, SDI-12	$SDI = 0.05 + 0.88\ SPI$	0.528
			$SDI = 0.04 + 0.87\ SPI + 0.01\ SPI^2$	0.528
			$SDI = 0.02 + 0.95\ SPI + 0.06\ SPI^2 - 0.03\ SPI^3$	0.53
		SPEI-12, SDI-12	$SDI = -0.10 + 0.87\ SPEI + 0.17\ SPEI^2$	0.522
			$SDI = -0.10 + 0.91\ SPEI + 0.17\ SPEI^2 - 0.02\ SPEI^3$	0.523
	Pud	SPI-12, SSI-12	$SSI = -0.12 + 0.77\ SPI$	0.53
			$SSI = -0.11 + 0.86\ SPI - 0.11\ SPI^2$	0.552
			$SSI = -0.03 + 0.97\ SPI - 0.04\ SPI^2 - 0.04\ SPI^3$	0.556
		SPEI-12, SSI-12	$SSI = -0.12 + 0.81\ SPEI$	0.554
			$SSI = -0.1 + 0.81\ SPEI - 0.02\ SPEI^2$	0.554
			$SSI = -0.1 + 0.83\ SPEI - 0.01\ SPEI^2 - 0.01\ SPEI^3$	0.555
		SPI-9, SDI-9	$SDI = -0.1 + 0.97\ SPI - 0.04\ SPI^2 - 0.77\ SPI^3$	0.504
		SPI-12, SDI-12	$SDI = -0.15 + 0.77\ SPI$	0.526
			$SDI = -0.03 + 0.87\ SPI - 0.12\ SPI^2$	0.552
			$SDI = -0.06 + 0.99\ SPI - 0.04\ SPI^2 - 0.05\ SPI^3$	0.556
		SPEI-9, SDI-9	$SDI = -0.13 + 0.77\ SPEI$	0.503
			$SDI = -0.14 + 0.77\ SPEI + 0.01\ SPEI^2$	0.503
			$SDI = -0.14 + 0.83\ SPEI + 0.02\ SPEI^2 - 0.03\ SPEI^3$	0.504
		SPEI-12, SDI-12	$SDI = -0.15 + 0.81\ SPEI$	0.553
			$SDI = -0.13 + 0.82\ SPEI - 0.02\ SPEI^2$	0.554
			$SDI = -0.13 + 0.86\ SPEI - 0.02\ SPEI^2 - 0.02\ SPEI^3$	0.555
	Pul	SPEI-12, SSI-12	$SSI = 0.13 + 0.31\ SPEI - 0.18\ SPEI^2 - 0.14\ SPEI^3$	0.52
			$SDI = 0.08 + 0.35\ SPEI - 0.18\ SPEI^2 + 0.14\ SPEI^3$	0.515

CONCLUSION

Once a perennial tropical river, the Bharathapuzha has become water-stressed in recent decades. This accentuates the necessity of monitoring for hydrological drought in the river basin. This study has utilised the capabilities of drought indices to understand the temporal and spatial extent of hydrological drought. The propagation of meteorological to hydrological droughts was also assessed in the study. The study assessed hydrological and meteorological drought events in the basin. During the summer and monsoon months of the year, decadal variation revealed a slight reduction in hydrological drought. According to the data analysed, droughts were most severe from 1988 to 1992 and 1999 to 2005. The highest severity observed was at Pudur, and the most extended drought duration observed was 70 months. The longest overall drought in the river basin lasted 64.90% of its observed period, encompassing mild to extreme drought occurrences. According to the cross-over correlation study, the meteorological stations that influence the hydrological stations are highly related on a 12-month timescale.

Furthermore, as per the literature, meteorological droughts are strongly linked to hydrological droughts over 12-month periods (Li *et al.* 2020a). A better response in the propagation of meteorological to hydrological drought was found within

a lag period of zero to three months. The research shows that the SPI-SSI and SPEI-SSI results are nearly identical, with minor differences where SPEI values are relatively higher. A similar observation is made with SPI-SDI and SPEI-SDI. The inclusion of potential evapotranspiration in SPEI may have resulted in a slight rise in values. The relation between meteorological and hydrological drought was established using nonlinear polynomial models, of which cubic models gave the highest coefficient of determination, followed by quadratic and linear models. Integrating other drought triggering components of the hydrological cycle and sophisticated advanced techniques would give more insight into these research dimensions.

DATA AVAILABILITY STATEMENT

All relevant data are available from the streamflow data provided by the Central Water Commission (CWC) is freely available (see: https://indiawris.gov.in/wris/#/RiverMonitoring). The precipitation and temperature data provided by the Indian Meteorological Department, Pune, is also freely available (see: https://www.imdpune.gov.in/Clim_Pred_LRF_New/Grided_Data_Download.html).

REFERENCES

Ahmadalipour, A., Moradkhani, H. & Demirel, M. C. 2017 A comparative assessment of projected meteorological and hydrological droughts: elucidating the role of temperature. *Journal of Hydrology* **553**, 785–797.

Apurv, T., Sivapalan, M. & Cai, X. 2017 Understanding the role of climate characteristics in drought propagation. *Water Resources Research* **53** (11), 9304–9329.

Dai, A. 2011 Characteristics and trends in various forms of the Palmer Drought Severity Index during 1900–2008. *Journal of Geophysical Research: Atmospheres* **116** (D12).

Drissia, T. K. 2019 Spatial and temporal variation of water stress in Bharathapuzha River basin, Kerala, India. *Journal of The Institution of Engineers (India): Series A* **100** (1), 167–175.

Edossa, D. C., Babel, M. S. & Gupta, A. D. 2010 Drought analysis in the Awash River basin, Ethiopia. *Water Resources Management* **24** (7), 1441–1460.

Eslamian, S., Ostad-Ali-Askari, K., Singh, V. P., Dalezios, N. R., Ghane, M., Yihdego, Y. & Matouq, M. 2017 A review of drought indices. *International Journal of Constructive Research in Civil Engineering* **3**, 48–66.

Katipoğlu, O. M., Acar, R. & Şenocak, S. 2021 Spatio-temporal analysis of meteorological and hydrological droughts in the Euphrates Basin, Turkey. *Water Supply* **21** (4), 1657–1673.

Li, Q., He, P., He, Y., Han, X., Zeng, T., Lu, G. & Wang, H. 2020a Investigation to the relation between meteorological drought and hydrological drought in the upper Shaying River Basin using wavelet analysis. *Atmospheric Research* **234**, 104743.

Li, R., Chen, N., Zhang, X., Zeng, L., Wang, X., Tang, S. & Niyogi, D. 2020b Quantitative analysis of agricultural drought propagation process in the Yangtze River Basin by using cross wavelet analysis and spatial autocorrelation. *Agricultural and Forest Meteorology* **280**, 107809.

Lindsay, J., Dean, A. J. & Supski, S. 2017 Responding to the Millennium drought: comparing domestic water cultures in three Australian cities. *Regional Environmental Change* **17** (2), 565–577.

Lotfirad, M., Esmaeili-Gisavandani, H. & Adib, A. 2022 Drought monitoring and prediction using SPI, SPEI, and random forest model in various climates of Iran. *Journal of Water and Climate Change* **13** (2), 383–406.

Malik, A., Kumar, A., Salih, S. Q. & Yaseen, Z. M. 2021 Hydrological drought investigation using streamflow drought index. In: *Intelligent Data Analytics for Decision-Support Systems in Hazard Mitigation* (Deo, R., Samui, P., Kisi, O. & Yaseen, Z. (eds)), Springer, Singapore, pp. 63–88. See: https://doi.org/10.1007/978-981-15-5772-9_4.

Mazrooei, A., Sinha, T., Sankarasubramanian, A., Kumar, S. & Peters-Lidard, C. D. 2015 Decomposition of sources of errors in seasonal streamflow forecasting over the US Sunbelt. *Journal of Geophysical Research: Atmospheres* **120** (23), 11–809.

McCleskey, R. B., Nordstrom, D. K., Susong, D. D., Ball, J. W. & Holloway, J. M. 2010 Source and fate of inorganic solutes in the Gibbon River, Yellowstone National Park, Wyoming, USA: I. Low-flow discharge and major solute chemistry. *Journal of Volcanology and Geothermal Research* **193** (3–4), 189–202.

Mckee, T. B., Doesken, N. J. & Leist, J. 1993 The relationship of drought frequency and duration to time scales. In: *Preprints 8th Conference on Applied Climatology*. Vol. 17, pp. 179–184.

Mishra, A. K. & Singh, V. P. 2010 A review of drought concepts. *Journal of Hydrology* **391** (1–2), 202–216.

Mishra, V., Tiwari, A. D., Aadhar, S., Shah, R., Xiao, M., Pai, D. S. & Lettenmaier, D. 2019 Drought and famine in India, 1870–2016. *Geophysical Research Letters* **46** (4), 2075–2083.

Mishra, V., Thirumalai, K., Singh, D. & Aadhar, S. 2020 Future exacerbation of hot and dry summer monsoon extremes in India. *npj Climate and Atmospheric Science* **3** (1), 1–9.

Modarres, R. 2007 Streamflow drought time series forecasting. *Stochastic Environmental Research and Risk Assessment* **21** (3), 223–233. doi:10.1007/s00477-006-0058-1.

Nalbantis, I. & Tsakiris, G. 2009 Assessment of hydrological drought revisited. *Water Resources Management* **23** (5), 881–897.

Rose, J. & Chithra, N. R. 2020 Evaluation of temporal drought variation and projection in a tropical river basin of Kerala. *Journal of Water and Climate Change* **11** (S1), 115–132.

Salimi, H., Asadi, E. & Darbandi, S. 2021 Meteorological and hydrological drought monitoring using several drought indices. *Applied Water Science* **11** (2), 1–10.

Van Loon, A. F. 2015 Hydrological drought explained. *Wiley Interdisciplinary Reviews: Water* **2** (4), 359–392.

Vasiliades, L., Loukas, A. & Liberis, N. 2011 A water balance derived drought index for Pinios River Basin, Greece. *Water Resources Management* **25** (4), 1087–1101.

Vicente-Serrano, S. M., Beguería, S. & López-Moreno, J. I. 2010 A multiscalar drought index sensitive to global warming: the standardized precipitation evapotranspiration index. *Journal of Climate* **23** (7), 1696–1718.

Vidal, J. P., Martin, E., Franchistéguy, L., Habets, F., Soubeyroux, J. M., Blanchard, M. & Baillon, M. 2010 Multilevel and multiscale drought reanalysis over France with the Safran-Isba-Modcou hydrometeorological suite. *Hydrology and Earth System Sciences* **14** (3), 459–478.

Wable, P. S., Jha, M. K. & Shekhar, A. 2019 Comparison of drought indices in a semi-arid river basin of India. *Water Resources Management* **33** (1), 75–102.

Wilhite, D. A. 2000 Drought as a natural hazard: concepts and definitions. In: *Drought: A Global Assessment*, Wilhite, D. A. (ed.), Vol. I, chap. 1. Routledge, London, pp. 3–18

First received 10 November 2021; accepted in revised form 31 January 2022. Available online 11 February 2022